Congresso de Métodos Numéricos em Engenharia
1-3 julho 2019, Guimarães, Portugal
Universidade do Minho

AN ANALYTICAL MODEL FOR THE TEXTILE-TO-MORTAR BOND BEHAVIOUR

A. Dalalbashi[1], B. Ghiassi[2] and D.V. Oliveira[3]

1: Department of Civil Engineering, ISISE & IB-S
School of Engineering, University of Minho
e-mail: alidalalbashi@gmail.com

2: Centre for Structural Engineering and Informatics
Faculty of Engineering, University of Nottingham
e-mail: bahman.ghiassi@nottingham.ac.uk

3: Department of Civil Engineering, ISISE & IB-S
School of Engineering, University of Minho
e-mail: danvco@civil.uminho.pt

Keywords: Bond behaviour, textile-reinforced mortar, pull-out test, shear stress bond-slip law

Abstract *Non-traditional retrofitting and strengthening, such as textile-reinforced mortar systems (TRMs), have recently received extensive attention for seismic protection of masonry and historical structures. One of the most important parameters in TRM-strengthened masonry is the bond behaviour of textile-to mortar and* mortar-*to-substrate. Although in the literature there are some researches about the bond behaviour between TRM and substrate, few attention has been paid to the bond of textile-to-mortar under pull-out test.*

An analytical model simulating the bond behaviour of textile-to-mortar composites is presented to relate the mechanical properties of the mortar and the textile as well as the load-slip curve gained from the pull-out tests. The objective of this study is to obtain the bond-slip law of different textile configurations and embedded lengths. In the formulation of the pull-out model, a modified approach based on a mathematical model by Banholzer is applied. Firstly, based on the experimental results and material properties, a relationship between the bond shear stress and the relative slip along the fiber-mortar interface is obtained.

1. INTRODUCTION

Nowadays, Textile Reinforced Mortar (TRM) composites have been very interesting possibilities for the externally bonded reinforcement (EBR) of masonry and reinforced concrete (RC) structures. TRMs composed of continuous fibers embedded in a matrix are used with a variety of unidirectional and bidirectional fibers and mortar types, which makes the development of unified design relations for these materials a complicated task. Glass, steel and basalt are among the most common fiber types used, while for the matrix, cementitious or lime-based mortars are usually used. Lime-based mortars are preferred for application to masonry and historical structures due to compatibility, sustainability issues, breathability and capability of accommodating structural movements [1–3].

The effectiveness of this strengthening technique is strongly dependent on the nonlinear properties of the TRM composite and on the mortar-to-substrate bond properties. At the same time, the nonlinear properties of TRMs are dependent on the fiber and mortar properties as well as fiber-to-mortar bond behavior. While most of the attention has been given to the tensile response of TRMs and to the TRM-to-substrate bond behavior, the fiber-to-mortar bond response is relatively unknown and poorly addressed [4–7].

In order to better understand the bond behavior between fiber and mortar in TRM system and proposing suitable bond-slip laws, it is presented here an analytical study on the effect of fiber-embedded length and configuration on the bond response of these composites.

2. ANALYTICAL MODELING

Two different models based on stress approach are addressed in the literature for analyzing the bond behavior between fiber and matrix: the perfect and the cohesive interface model [8]. The perfect interface model is based on linear elastic model and usually used for composite materials such as fiber and resin matrix, in which no slip between reinforcing element and matrix is allowed [8]. The cohesive or imperfect interface model is usually utilized for analyzing the bond between fiber and lime/cement-based matrix [8]. In this model, three material composites are considered for investigation of bond behavior of fiber-to-matrix: reinforcing element, matrix, and the imperfect interface between fiber and matrix obtained indirectly from the pull-out response [9].

The assumed mechanism in the cohesive interface model under pull-out test is divided into three stages: elastic, nonlinear, and dynamic stages [6,10,11]. In the elastic stage, a perfect or adhesive bond exists between fiber and matrix. By increasing the pull-out force, the progressive destruction of the adhesive bond occurs and hence debonding takes place when the maximum stress is reached at the interface (nonlinear stage). After complete debonding along the embedded length of fiber, the only resisting mechanism is friction between the fiber and the matrix (dynamic stage). Hence, various proposal bond-slip law models about the bond stress versus slip relation have been made (Figure 1). The first proposed model is considered the stress-slip relation to consist of a linear elastic part followed by a sudden stress drop and a residual constant friction or exponential decay friction, as shown in Figure 1a, [6,10,11]. A second bond-slip law model assumes that the relation between stress and slip is a nonlinear curve (N-piecewise model), as shown in Figure 1b, [8,12].

In the current study, the bond-slip law is assumed multi-linear and is obtained indirectly from the experimental pull-out curves following the model proposed by Banholzer et al. [8,12]. In this model, the experimental load-slip curve is divided into n steps. From the experimental

test, the pull-out load, P_n, and its corresponding fiber slip, ω_n, are known for each load step. The parameters γ and q, defined as the relative compliance and the normalized pull-out force, respectively, are obtained as follows:

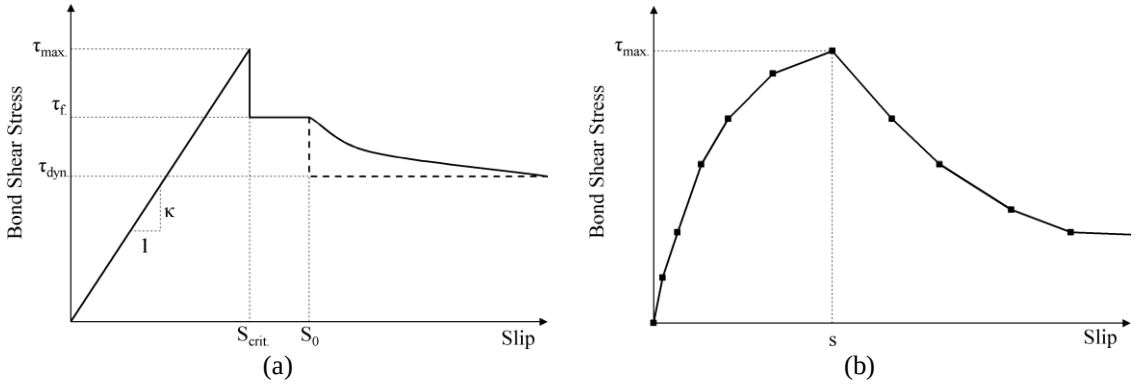

Figure 1. Proposed bond shear stress versus slip relationship.

$$\gamma = \frac{1}{A_f E_f} + \frac{1}{A_m E_m} \tag{1}$$

$$q = \gamma P \tag{2}$$

Where A is the cross-sectional area and E is the Young's modulus. The subscripts f and m refer to the fiber and the matrix, respectively. The bond stress, τ_s, and its corresponding slip, S, are normalized for simplicity in terms of T_s, which is calculated as:

$$T_s = m_i \left(S - S_{i-1}\right) + T_{i-1} = \pi d \gamma \tau_s \tag{3}$$

Where, S_{i-1} is the slip at the lower bond of an interval i of the piecewise defined normalized shear flow versus slip relation. T_{i-1} and d are the normalized shear flow corresponding to the slip S_{i-1} and the fiber diameter, respectively. m_i is the slope of the N-piecewise linear normalized shear flow-slip relation in an interval i and is equal to:

$$m_i = \frac{T_i - T_{i-1}}{S_i - S_{i-1}}, \; T_0 = S_0 = 0 \tag{4}$$

The procedure is to find the shear stress distribution, τ_n, or the normalized shear flow, T_n, along the bonded length in each step. T_n has to be found in an iterative procedure for a given slip $\omega = S$ at $x = L$ and a given pull-out force $P = \gamma^{-1} q$. For each load step, n, the introduced slip and its corresponding pull-out load are known from the experimental tests. The procedure for finding the bond-slip law can be summarized as follows:

1) At $n = 1$, P_1 and S_1 are known from the experimental results, thereby T_1 can be calculated from the following equation:

$$L = \frac{1}{\sqrt{m_k}} \ln\left[\frac{\sqrt{m_k} q_k + T_k}{\sqrt{T_k^2 - m_k q_k^2}}\right] = \frac{1}{\sqrt{m_1}} \ln\left[\frac{\sqrt{m_1} q_1 + T_1}{\sqrt{T_1^2 - m_1 q_1^2}}\right] \tag{5}$$

L and q are the embedded length of fiber and normalized force in the fiber at location x ($q_1 = \gamma P_1$), respectively. Based on Eq. (4), m_1 depends on T_1 that is the only unknown

parameter in Eq. (5). The subscript k refers to the point in which the force in the fiber is zero [8].

2) To determine T_2, a value should be initially assumed. Then from Eq. (4), the value of m_2 is calculated. By obtaining m_2, the following equation can be solved:

$$\begin{aligned} q_{i-1}^2 &= q_i^2 - m_i\left(S_i - S_{i-1}\right)^2 - 2T_{i-1}\left(S_i - S_{i-1}\right) \Rightarrow \\ q_1^2 &= q_2^2 - m_2\left(S_2 - S_1\right)^2 - 2T_1\left(S_2 - S_1\right) \end{aligned} \tag{6}$$

If the obtained value of Eq. (6) is negative, then the assumed value is correct and one can proceed to the next step. Otherwise, the value of T_2 must be changed so that the amount of Eq. (6) becomes negative. Therefore, this recursive determination of the fiber forces guarantees that there is a point in which the fiber load is zero [8].

3) The accurate value for T_2 is obtained by solving the following equation:

$$L = \overline{\Delta x} + \sum_{i=k+1}^{n} \Delta x_i \tag{7}$$

where $\overline{\Delta x}$ and Δx_i can be determined as follows:

$$\begin{aligned} \overline{\Delta x} &= \frac{1}{\sqrt{m_k}} \ln\left[\frac{\sqrt{m_k}\,q_k + T_k}{\sqrt{T_k^2 - m_k q_k^2}}\right], && m_k > 0 \\ \overline{\Delta x} &= \frac{1}{\sqrt{-m_k}} \arcsin\left[\frac{\sqrt{-m_k}\left(-q_k\sqrt{T_k^2 - m_k q_k^2}\right)}{T_k^2 - m_k q_k^2}\right], && m_k < 0 \end{aligned} \tag{8}$$

$$\begin{aligned} \overline{\Delta x_i} &= \frac{1}{\sqrt{m_i}} \ln\left[\frac{\sqrt{m_i}\,q_i + T_i}{\sqrt{m_i}\,q_{i-1} + T_{i-1}}\right], && m_i > 0 \\ \overline{\Delta x} &= \frac{1}{\sqrt{-m_i}} \arcsin\left[\frac{\sqrt{-m_i}\left(T_i q_{i-1} - T_{i-1} q_i\right)}{T_{i-1}^2 - m_k q_{i-1}^2}\right], && m_i < 0 \end{aligned} \tag{9}$$

In fact, by solving Eq. (6), the precise point of the embedded length in which the fiber load is equal to zero is obtained [8].

4) Having T_2, the shear stress is calculated by Eq. (3).

5) This procedure is then repeated for the next steps (n= 3, 4 …).

The main input parameters required for this problem are the elastic modulus of the fiber and the mortar that are usually known from the experimental tests, and the mortar load carrying area. This latter has not been determined explicitly in the literature [12–15]. The effect of this parameter on the bond-slip laws has been previously discussed by the authors in [11]. The results illustrated that as the mortar effective area changes, the bond strength, bond shear modulus, and friction stress vary significantly. As suggested in [11], the effective mortar area in this study is considered equal to 55 times of the fiber area for all the specimens, in order to compare the obtained results with the previous study. This value is obtained based on satisfying the following convergence criteria: solving differential equations of force equilibrium at the interface of fiber and mortar, calculating the bond parameters, and verifying

the analytical load-slip curve with experimental curve. The parametric study illustrated that the mortar area can be selected between 55 and 100 times the fiber area, though 55 yielded a more accurate answer and it was chosen for the simulations [11].

3. EXTRACTING BOND-SLIP LAW

In order to obtain bond-slip law of fiber-to-mortar, the results of pull-out tests conducted by authors are used [16]. The test setup consisted in pull-push configuration to perform pull-out test (Figure 2). In this experimental campaign, the steel fibers with different embedded length and configurations as well as hydraulic lime-based mortar are tested. Fiber bond lengths are equal to 50, 100, 150, and 200 mm. In addition, the force-slip of single fiber, double fiber, and group fiber (four fibers) have been reported in which the bond length are 150 mm. The elastic modulus of the fiber and its area are equal to 189.34 GPa and 0.538 mm^2, respectively. Also, the compression elastic modulus of mortar is reported to be 9.0 GPa.

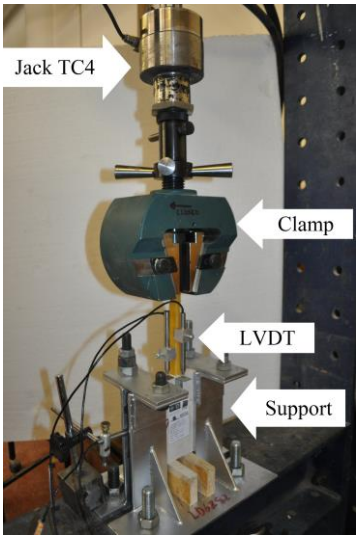

Figure 2. Test setup and instrumentation used for pull-out tests.

3.1. Bond slip-law based on bond length

The average bond-slip laws obtained with the aim of the N-piecewise model for different embedded lengths are shown in Figure 3 and Table 1. Interestingly, the average bond-slip laws are similar (with slight differences) in all embedded lengths. The bond strength is obtained in the range of 3.1-3.6 MPa in embedded lengths smaller than 150 mm and slightly smaller in the embedded length of 200 mm (2.3 MPa). It seems that the shear stiffness of the bond-slip law, κ, decreases (and consequently the slip corresponding to the bond strength increases) with increment of the embedded length. Finally, the residual part of the bond slip law is most probably related to the frictional effect.

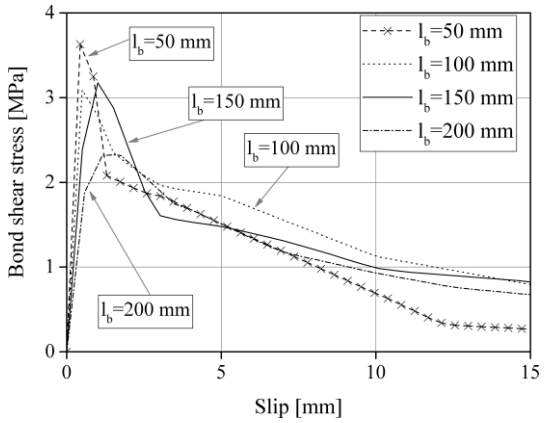

Figure 3. Average of bond stress-slip law diagram of single steel fiber with different embedded length.

Specimen	l_b=50 mm	l_b=100 mm	l_b=150 mm	l_b=200 mm	Double fiber	Group fiber
τ_{max} [MPa]*	3.6	3.1	3.2	2.3	3.1	2.8
S_{max} [N]*	0.4	0.5	1.0	1.7	1.0	1.0
κ [N/mm^3]*	8.4	6.7	5.0	3.4	5.6	5.6

* τ_{max}: Maximum shear stress, S_{max}: slip corresponding to maximum shear stress, κ: bond modulus.

Table 1. Bond-slip law properties in steel-based TRM.

3.2. Bond slip-law based on fiber configuration

The analytical bond-slip laws are presented in Figure 4 and Table 2. The analytical modeling of the group steel fibers assumes that a uniform load is applied to all fibers owing to the epoxy resin block; thus, the obtained load from the experimental test is divided by the number of fibers. This assumption seems acceptable when deriving average bond-slip laws for the TRM composites is of concern. The analytical results show that the number of steel fibers does not have a significant influence on the shear modulus and bond strength in the bond-slip laws, as shown in Figure 4 and Table 2. It can be observed that although the pull-out response of single and double fiber specimens show a different behavior after complete debonding (see Figure 4), the frictional stresses of these specimens are approximately the same. The frictional stress of the group fibers, however, is smaller than the single and the double fiber specimens, which can be attributed to the distributed cracking of the mortar in these specimens. Consequently, by increasing the number of fibers, the failure mode changes from pull-out to mortar cracking. Moreover, the more the number of fiber, the more cracking in the mortar; as a result, both peak load and frictional stress decrease.

Specimen	Slip corresponding to peak load [mm]	Peak load/ per fiber [N]	Toughness until peak load/ per fiber [N.mm]	Initial stiffness/ per fiber [N/mm]
Single-fiber	1.08 (17.6)	992 (9.8)	730 (23.2)	2772 (18.2)
Double fiber	0.89 (26)	815 (14.2)	538 (29.8)	2863 (30.3)
Group fiber	0.74 (43.8)	700 (15)	340 (57.1)	2058 (61.6)

*CoV of the results are given in percentage inside parentheses

Table 2. Changes of bond properties in steel-based TRM with fiber configuration.*

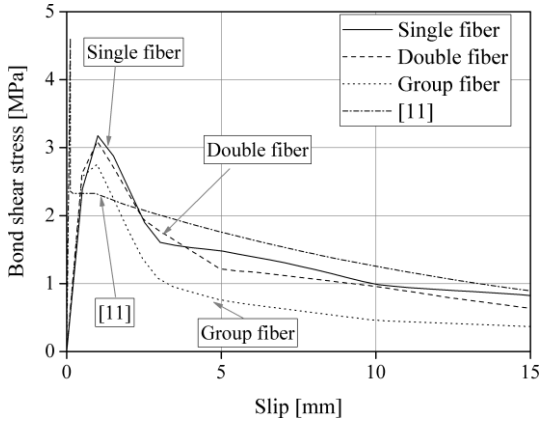

Figure 4. Average of bond stress-slip law diagram of steel fiber with different configuration.

A comparison between the bond-slip laws obtained from the method used in [11] and that of obtained in the current study for the single steel fiber with 150 mm embedded length, Figure 4 and Table 3, shows that the results are significantly dependent on the adapted approach. These differences that are rooted on the analysis method and the assumptions made show that the solution to the mathematical problem of delamination is not unique and different solutions (bond-slip laws) can be obtained when different approaches are followed. In the model utilized in the current study, the pull-out problem is expressed with respect to the slip distribution over the embedded length [8,12], while the model used by the authors in [11], is expressed based on the local shear stresses [10,11].

Method	κ [N/mm^3]	τ_{max} [N/mm^2]	Slip at full debonding [mm]	Slip corresponding to the τ_{max} [mm]
multi-linear bond-slip law proposed by [11]	39.5	4.6	0.92	0.12
N-piecewise model	5.0	3.2	-	1.0

Table 3. Comparing the bond-slip law between two different methods in M2-SS1-150 specimens.

4. CONCLUSIONS

In this study with the aim of proposing suitable bond-slip laws for steel-based TRM systems, an analytical investigation is presented. Therefore, the effect of bond length and fiber configuration on the fiber-to-mortar bond response in these composites is deeply investigated. In general, it is observed that bond-slip laws obtained from the pull-out tests are not significantly different for different embedded lengths unless a different failure mode occurred. In addition, the bond-slip laws of steel fiber with different configurations are approximately in the elastic region (until the bond strength). The frictional stress however is decreased by increasing the number of fibers.

5. ACKNOWLEDGEMENT

This work was partly financed by FEDER funds through the Operational Programme Competitiveness Factors (COMPETE 2020) and by national funds through the Foundation for Science and Technology (FCT) within the scope of project POCI-01-0145-FEDER-007633. The support to the first author through the grant SFRH/BD/131282/2017 is acknowledged.

6. REFERENCES

[1] S. Barr, W.J. Mccarter, B. Suryanto, *Bond-strength performance of hydraulic lime and natural cement mortared sandstone masonry*, Constr. Build. Mater. 84 (2015) 128–135. doi:10.1016/j.conbuildmat.2015.03.016.

[2] V. Pavlík, M. Uzáková, *Effect of curing conditions on the properties of lime, lime–metakaolin and lime–zeolite mortars*, Constr. Build. Mater. 102 (2016) 14–25. doi:10.1016/j.conbuildmat.2015.10.128.

[3] C. Groot, RILEM TC 203-RHM: *Performance requirements for renders and plasters*, Mater. Struct. 45 (2012) 1277–1285. doi:10.1617/s11527-012-9916-0.

[4] J. Yu, J. Yao, X. Lin, H. Li, J.Y.K. Lam, C.K.Y. Leung, I.M.L. Sham, K. Shih, *Tensile performance of sustainable Strain-Hardening Cementitious Composites with hybrid PVA and recycled PET fibers*, Cem. Concr. Res. 107 (2018) 110–123. doi:10.1016/j.cemconres.2018.02.013.

[5] E. Grande, M. Imbimbo, E. Sacco, *Numerical investigation on the bond behavior of FRCM strengthening systems*, Compos. Part B. 145 (2018) 240–251. doi:10.1016/j.compositesb.2018.03.010.

[6] B. Ghiassi, D. V Oliveira, V. Marques, E. Soares, H. Maljaee, *Multi-level characterization of steel reinforced mortars for strengthening of masonry structures*, Mater. Des. 110 (2016) 903–913. doi:10.1016/j.matdes.2016.08.034.

[7] A. Bilotta, F. Ceroni, G.P. Lignola, A. Prota, *Use of DIC technique for investigating the behaviour of FRCM materials for strengthening masonry elements*, Compos. Part B Eng. 129 (2017). doi:10.1016/j.compositesb.2017.05.075.

[8] B. Banholzer, *Analytical simulation of pull-out tests- the direct problem*, Cem. Concr. Compos. 27 (2005) 93–101. doi:10.1016/j.cemconcomp.2004.01.006.

[9] P. Lawrence, *Some theoretical considerations of fibre pull-out from an elastic matrix*, J. Mater. Sci. 7 (1972) 1–6. doi:10.1007/BF00549541.

[10] A.E. Naaman, G.G. Namur, J.M. Alwan, H.S. Najm, *Fiber pullout and bond slip. i: analytical study*, J. Struct. Eng. 117 (1991) 2769–2790. doi:10.1061/(ASCE)0733-9445(1991)117:9(2769).

[11] A. Dalalbashi, B. Ghiassi, D.V. Oliveira, A. Freitas, *Effect of test setup on the fiber-to-mortar pullout response in TRM composites: experimental and analytical modeling*, Compos. Part B Eng. 143 (2018) 250–268. doi:10.1016/j.compositesb.2018.02.010.

[12] B. Banholzer, W. Brameshuber, W. Jung, *Analytical evaluation of pull-out tests-The inverse problem*, Cem. Concr. Compos. 28 (2006) 564–571. doi:10.1016/j.cemconcomp.2006.02.015.

[13] B. Mobasher, *Mechanics of Fiber and Textile Reinforced Cement Composites*, Taylor & Francis Group, London- New York, 2012.

[14] J.M. Alwan, A. Naaman, W. Hansen, *Pull-Out work of steel fibers from cementitious composites : analytical investigation*, Cem. Concr. Compos. 13 (1991) 247–255. doi:10.1016/0958-9465(91)90030-L.

[15] C. Sujivorakul, A.M. Wass, A.E. Naaman, *Pullout response of a smooth fiber with an end anchorage*, J. Eng. Mech. 126 (2000) 123–131. doi:10.1061/(ASCE)0733-9399(2000)126:9(986).

[16] A. Dalalbashi, B. Ghiassi, D.V. Oliveira, A. Freitas, *Fiber-to-mortar bond behavior in TRM composites: effect of embedded length and fiber configuration*, Compos. Part B Eng. 152 (2018) 43–57. doi:10.1016/j.compositesb.2018.06.014.